Temporal Evolution of Nanoscale Structures in Ni-Based Superalloys

Undergraduate Researcher
Luis de la Cruz, Lehigh University,
Bethlehem, Pennsylvania

Faculty Mentor
David Seidman
Department of Materials Science and Engineering,
Northwestern University

Postdoctoral Mentor
Dieter Isheim
Department of Materials Science and Engineering,
Northwestern University

Graduate Student Mentor
Chantal Sudbrack
Department of Materials Science and Engineering,
Northwestern University

Abstract

The effects of Ru, W, and Re on the temporal evolution of the gamma prime precipitates in a Ni-Cr-Al alloy were investigated by three-dimensional atom probe (3DAP) microscopy. The spatial distribution of the gamma prime precipitates in a model Ni-8.5Cr-10Al alloy was investigated using atomic force microscopy (AFM). We reported on the alloys' Ni-8.5Cr-10Al-2Ru atomic percent (at%), Ni-8.5Cr-10Al-1Ru-1Re at%, and Ni-8.5Cr-10Al-0.5Ru-0.5Re-1W at%, which were aged isothermally in the gamma/gamma prime two-phase field at 1073K for 4 and 16 hours each. We also reported on a Ni-8.5Cr-10Al alloy, which also was aged isothermally in the gamma/gamma prime two-phase field at 1073K for 15-minute, one-hour, and four-hour periods. A sample for this alloy that was not aged or quenched also was investigated.

The partitioning and spatially resolved phase concentrations across the gamma prime precipitates and gamma matrix were obtained from the 3DAP reconstructions. At the concentrations studied, the addition of Re to the NiCrAlRu alloy had little influence on the partitioning ratios of Ni, Al, Cr, and Ru. The addition of W to the NiCrAlRuRe alloy did not affect the partitioning ratios of Ni, Re, and Ru but did cause stronger partitioning of Cr to the matrix and Al to the precipitate. The number densities calculated from the AFM images for the model Ni-8.5Cr-10Al alloy for the zero-hour, 15-minute, one-hour, and four-hour aging times were 3.91×10^{22}, 1.48×10^{22}, 2.88×10^{21}, and 9.83×10^{20} m^{-3}, respectively.

Introduction

Superalloy is a term widely used by engineers to characterize a group of metallic alloys specifically designed to function at elevated temperatures.[1] These alloys must serve where high stresses (e.g., tensile, fatigue, and thermal) are applied in combination with high oxidation resistance.[1] The driving force for development of these complex nickel-based superalloys is the improved performance of land-based gas turbines and aviation jet engines.[2] Current commercial superalloys (third-generation superalloys), including Rene N6 and CMSX-10, are composed of 12 or 13 alloying elements.[2] Refractory elements are added because they strengthen the matrix as well as the precipitates, but the main reason is to increase the melting point of the material. The addition of alloying elements also can reduce the lattice misfit between the matrix and coherent precipitates.

Ni-Cr-Al-based alloys are among the most popular Ni-based superalloys because of their excellent mechanical properties at very high temperatures. Their strength at very high temperatures is owed to the presence of LI_2-ordered precipitates of Ni_3Al (gamma prime) in a face-centered (FCC), chromium-rich solid solution (gamma). The addition of Cr to the binary Ni-Al system significantly reduces the lattice parameter misfit between the precipitate and the matrix phase, which slows down the coarsening process.

In this study, the effects of W and Re on the decomposition behavior of a NiCrAl-based alloy that also contains Ru were studied. Ru has not been used before in commercial alloys, so the research examined the behaviors exhibited by W and Re when exposed to this new element. W and Re are an important part of the third-generation commercial alloys, especially Rene N6 and CMSX-10, where they contribute approximately 12% of the total weight.[2]

Three-dimensional atom probe (3DAP) microscopy was used to study the effect of the refractory elements mentioned above on the chemical composition and the coarsening behavior of gamma prime precipitates. The alloys investigated with the 3DAP were Ni-8.5Cr-10Al-2Ru at%, Ni-8.5Cr-10Al-1Ru-1Re at%, and Ni-8.5Cr-10Al-0.5Ru-0.5Re-1W at%.

The study also examined spatial distribution of the gamma prime precipitates in a model Ni-8.5Cr-10Al alloy for the aging times of zero hours, 15 minutes, one hour, and four hours using the AFM. Research focused on how the number density of the gamma prime precipitates evolves as a function of time.

The combination of both studies yields a thorough investigation of phase composition, precipitate size, and spatial distribution of the precipitates, providing information about their microstructure and insight into their mechanical behavior.

Background

Previous investigations proved that the addition of refractory elements increased strength and enhanced high-temperature properties.[3] Alloys containing these

		Matrix						Precipitate					
Alloy	t_{800oC}	Ni	Cr	Al	Ru	Re	W	Ni	Cr	Al	Ru	Re	W
2-10	4 h	80.82 0.56	9.34 0.43	7.86 0.04	1.97 0.02			76.20 0.09	5.75 0.05	17.2 0.08	0.77 0.02		
	16 h	81.21 0.08	9.00 0.06	7.80 0.05	1.98 0.03			76.45 0.20	5.87 0.12	16.85 0.18	0.85 0.05		
2-11	4 h	80.39 0.06	9.70 0.04	7.79 0.04	1.10 0.01	1.00 0.02		75.91 0.11	5.30 0.06	17.79 0.10	0.44 0.02	0.55 0.02	
	16 h	81.22 0.10	9.72 0.09	7.22 0.07	1.00 0.02	0.98 0.03		76.52 0.08	5.26 0.04	17.22 0.08	0.39 0.01	0.55 0.01	
2-12	4 h	81.63 0.09	9.89 0.09	6.12 0.09	0.55 0.01	0.45 0.01	0.61 0.03	75.88 0.36	4.18 0.12	18.44 0.35	0.25 0.03	0.27 0.05	1.24 0.06
	16 h	78.75 0.11	10.14 0.09	7.00 0.07	0.52 0.02	0.44 0.02	0.55 0.01	76.85 0.05	4.60 0.03	16.73 0.05	0.20 0.01	0.19 0.01	1.34 0.01

Table 1: Phase compositions of Ni-8.5Cr-10Al-2Ru (2-10), Ni-8.5Cr-10Al-1Ru-1Re (2-11), 2-10: Ni-8.5Cr-10Al-0.5Ru-0.5Re-1W (2-12).

refractory additions have been thoroughly investigated with a focus on microstructure.[4,5,6] By combining this knowledge with better engineering design of turbine blades, the maximum operational temperature of the blades has been increased 300K since the early 1980s.[2] Even so, there is little experimental knowledge of the effect of individual refractory elements on matrix/precipitate equilibria and decomposition.

A key limitation of previous investigations was a lack of instrumentation, and this investigation attempted to compensate for this deficiency. With 3DAP, precipitates and concentration gradients can be examined in real space on a nanometer scale. The equipment also provides an atom-by-atom reconstruction on three dimensions of the specimen examined.

The AFM also gave this investigation an advantage over previous work. With it, precipitates as small as 8 nm could be analyzed.

Approach

Alloy preparation and heat treatments are explained in detail in Sudbrack et al., 2003.[7]

Three-Dimensional Atom Probe Microscope (3DAP)

A blank of each alloy of approximately 300 µm in width was provided. The 3DAP tips were prepared by electropolishing a square blank (0.3 mm x 0.3 mm x 10 mm) with a solution of 10 vol % perchloric acid in acetic acid, with a voltage of 12 V_{dc} at room temperature. The goal was to get a thin (150 µm) and evenly etched tip. Once this goal was met, the next step was to create a very sharp apex, which entailed additional electropolishing with a 2 vol % percholoric acid in 2-butoxyethanol and the application of short pulses of lower voltages (12 V_{ac}–6.5 V_{ac}). Once the tip was etched to a radius of approximately 50 nm, it was ready for analysis.

With the tip positioned in the main chamber of the atom probe and ready for analysis, the imaging process began. Imaging by field-ion microscopy at 40K at a gauge pressure of 2.0 x 10^{-5} neon and by applying a voltage on the specimen (first images seen around 2kV) revealed the crystal structure, which allowed for proper alignment of the specimen for the 3DAP analysis. Since field evaporation is directly dependent on the crystallographic orientation, all of the analyses in the investigation were aligned with the 001 pole. Once aligned, 3DAP analysis was carried out by identifying field-evaporated atoms from the specimen by time-of-flight mass spectrometry.

After 3DAP analysis, a program called ADAM 1.5b13 was used to create an atom-by-atom reconstruction of the volume analyzed. From the reconstructions, the exact phase compositions and partitioning ratios could be determined.

Partitioning Ratios							
alloy	Aging time	Ni	Cr	Al	Ru	Re	W
NiCrAlRu	4h	0.94	0.62	2.19	0.39		
	16h	0.94	0.65	2.16	0.43		
NiAlCrRuRe	4h	0.94	0.55	2.28	0.40	0.55	
	16h	0.94	0.54	2.38	0.39	0.56	
NiAlCrRuReW	4h	0.93	0.42	3.01	0.45	0.6	2.03
	16h	0.97	0.45	2.39	0.38	0.43	2.44

Table 2: Partitioning ratios for every component in the superalloy.

Atomic Force Microscopy
The alloys were mounted in hot mounts, and then the surface was ground using 400-, 600-, 800-, and 1200-grit SiC papers, respectively. The mounted alloys were then polished with 9 µm, 6 µm, and 1 µm diamond abrasive and ultrasonically cleaned between polishing steps. The final polish was done with a noncrystallizing colloidal silica suspension. Once the samples were thoroughly cleaned and taken out of the mounts, the samples were etched using a 100 ml deionized H_2O, 0.5 g $K_2S_2O_5$ solution. The etching times for the Ni-8.5Cr-10Al alloy were as follows:

Aging Times	Etching Times
0 hours	7 seconds
0.25 hours	5 seconds
1 hour	12 seconds
4 hours	10 seconds

The gamma prime precipitates were then imaged in the AFM using a silicon conical tip with a 2 nm apex diameter with a frequency of 8-16 kHz. Once an image of the surface was achieved, the precipitates were manually counted. Those that intersected the edge of the micrograph were counted as halves. Then the areal density, N_A, was measured and the number of precipitates, N_V, was calculated by using the following equation: $N_V = 2/3*(N_A)^{3/2}$.

Results and Discussion

Three-Dimensional Atom–Probe Reconstructions
Three-dimensional atom-by-atom reconstructions for the Ni-8.5Cr-10Al-2Ru, Ni-8.5Cr-10Al-1Ru-1Re, and Ni-8.5Cr-10Al-0.5Ru-0.5Re-1W alloys after aging at 1073K for 4 hours and 16 hours are shown in Figure 1. Aluminum atoms are red, Cr atoms are turquoise, Ru atoms are yellow, Re atoms are purplish pink, W atoms are green, and Ni atoms are omitted for clarity. Comparing the 4- and 16-hour reconstructions, it is clear that growth in precipitate size (coarsening) occurs as the aging time increases. A comparison of the size of the precipitates in the NiCrAlRu and NiCrAlRuRe alloys indicates that the precipitates are bigger in the NiCrAlRuRe alloy. Therefore, the addition of Re makes the precipitates coarsen faster. In contrast, if the NiCrAlRu alloy is compared with the NiCrAlRuReW, the precipitates seem smaller in the NiCrAlRuReW alloy, showing that the addition of W slows the coarsening process. This observation is in agreement with earlier experiments[7] in which the addition of W slowed the coarsening process in the tertiary alloy Ni-8.5Cr-10Al.

Phase Compositions from 3D Reconstructions/Partitioning Ratios
Quantitative chemical information was obtained from the 3D reconstructions shown in Figure 1. This was achieved by

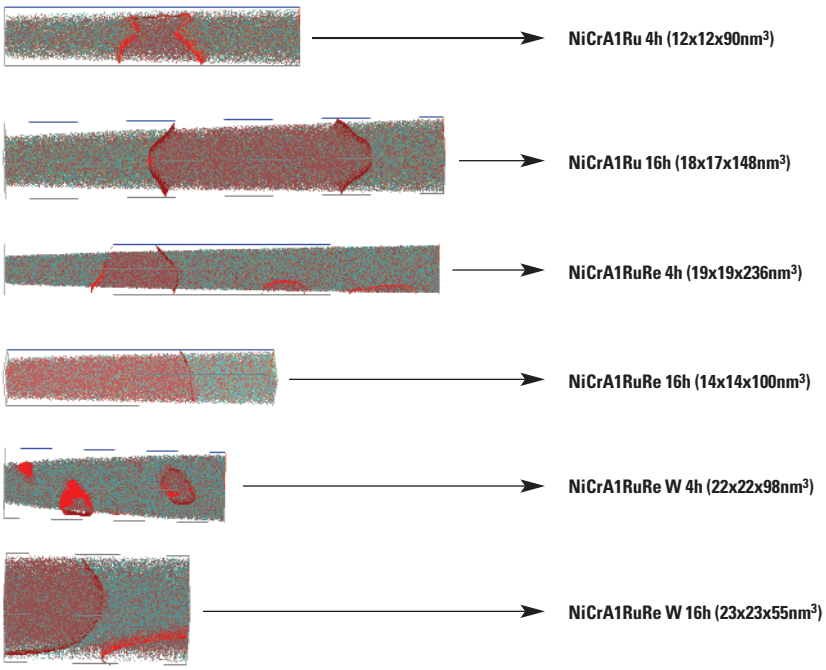

Figure 1: Atom-by-atom reconstructed volumes of the alloys studied by 3DAP.

delineating the gamma/gamma prime interface using an isoconcentration surface. The isoconcentration surface was defined by a threshold concentration of aluminum, in this case 12.75 at%. The threshold value was defined as the average of the mean Al concentration values in the matrix and precipitate away from the interface. Once the threshold value was established, ADAM 1.5b13 was used to calculate a proximity histogram (proxigram) for the 3D reconstructions. The proxigram allowed for determination of exact phase compositions by averaging the values that correspond to the matrix and the precipitate. Proxigrams are displayed in Figure 2, 3, and 4 for the NiCrAlRu, NiCrAlRuRe, and NiCrAlRuReW alloys, respectively.

The data converted to quantitative figures are shown in Table 1, which demonstrates the concentration of each component in the matrix and precipitate. Figure 5 represents the phase concentrations of the NiCrAlRu alloy for both aging times. (Ni is omitted because it acts as a balance in the alloy, and the study's focus was on the effect of the alloying elements.) The concentrations of Cr and Ru are higher in the matrix than the precipitate for both aging times, showing that Cr and Ru enrich in the matrix, or in more scientific terms, they partition to the matrix. In contrast, the concentration of Al is higher in the precipitate than the matrix. Therefore, Al is enriching the precipitate. Figure 6 represents the phase concentrations for the NiCrAlRuRe alloy (Ni is omitted) for both aging times. The refractory element added, Re, partitioned to the matrix for both aging times. Figure 7 shows the phase composition for the NiCrAlRuReW for both aging times, demonstrating that W partitions toward the precipitate, unlike Cr, Ru, and Re.

Partitioning ratios are defined as the concentration of the precipitate divided by the concentration of the matrix. The values for the partitioning ratios are shown in Table 2. A graphical representation of this data for the NiCrAlRu, NiCrAlRuRe, and NiCrAlRuReW alloys is shown in Figures 8, 9, and 10, respectively. When comparing Figures 8 and 9, it is clear that the addition of Re to the NiCrAlRu alloy does not affect the partitioning ratios of any of the elements. From this it can be concluded that, at the concentrations studied, the partitioning behaviors of Ru, Re, Cr, and Al are independent of each other. When comparing Figures 9 and 10, it is evident that the addition of W to the NiCrAlRuRe alloy has some effect on the partitioning behaviors of other elements within the alloy. The addition of W has caused a stronger partitioning of Cr to the matrix and of Al to the precipitate. This observation once again agrees with earlier work done by Sudbrack et al., 2003,[7] which found that the addition of W to a tertiary Ni-8.5Cr-10Al alloy caused stronger partitioning of Cr to the matrix and of Al to the precipitate. Although W causes a stronger partitioning in Al and Cr, it appears to have no effect on the partitioning ratios of Ru and Re. This is a somewhat positive outcome. Since the partitioning ratios of Ru, Re, and W are independent of each other, these elements can be added to an alloy that is designed in an additive manner.

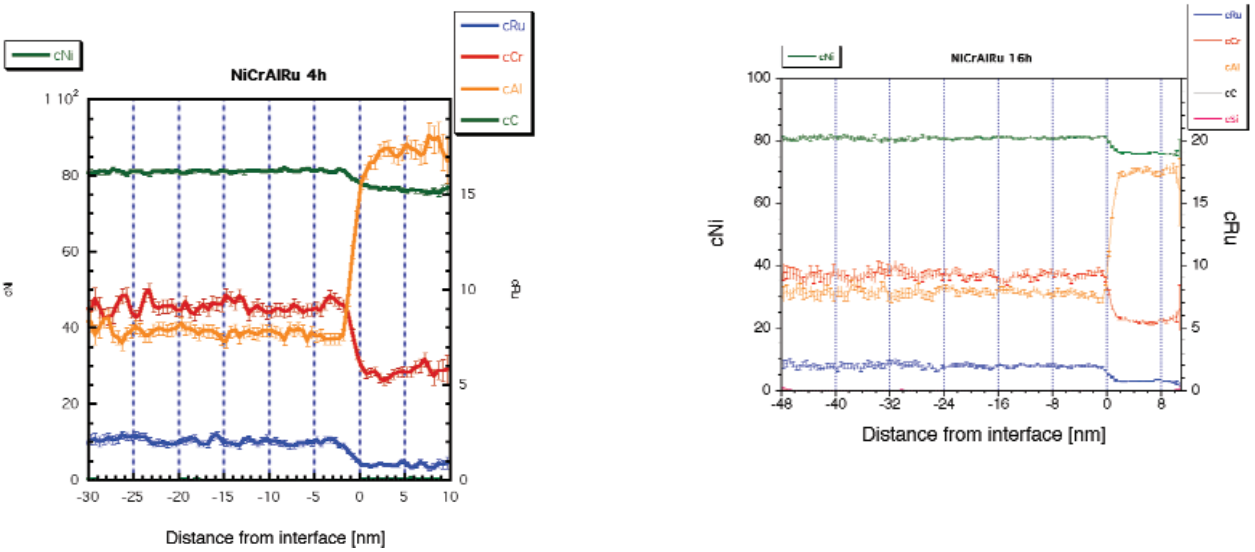

Figure 2: Proximity histograms for the Ni-8.5Cr-10Al-2Ru alloy.

Spatial Distribution from AFM Images
Gamma prime precipitates were imaged using AFM. Figure 11 shows images taken for the Ni-8.5Cr-10Al alloy for the zero-hour, 15-minute, one-hour, and four-hour aging times. (The image for the one-hour aging time has a better resolution than any of the other images because it was imaged with a different tip. This silicon tip was in very good condition but could not be used for the other aging times because it broke during an analysis. The other images were taken with a different silicon tip with a lower resolution. This demonstrates how crucial an AFM tip can be for analysis.)

Figure 11 shows that the alloy exhibits a change in the size and number density of the precipitates. From the images, it is clear that for the zero-hour aging time (as quenched) and the 15-minute aging time, precipitates seem small and randomly distributed. As the aging time is increased, so is the size of the precipitates — obvious coarsening is seen. (The process is clearly at the beginning stage of coarsening because the precipitates are still spherical in shape.) If the time is increased further, the later stages of coarsening, where the precipitates start to form a cuboidal shape, would be evident.

As the aging time is increased, the number density decreases. The values found for the zero-hour, 15-minute, one-hour, and four-hour aging times are 3.91 x 10^{22}, 1.48 x 10^{22}, 2.88 x 10^{21}, and 9.83 x $10^{20}m^{-3}$, respectively. In Figure 12, the number densities are plotted, creating a graph that also includes unpublished results by T. Ziebell and C. Sudbrack obtained by using transmission electron microscopy (TEM) and scanning electron microscopy (SEM).

This study's results, using the AFM, are in good agreement with the TEM and SEM results from past studies. Because of its better resolution, the AFM was able to produce images for the shorter aging times studied, something the SEM could not. By using these results and adding earlier results from past studies, it was possible to plot the number densities for the aging times ranging from zero hour to 264 hours. The plot shows a line with a downward slope of -0.91 — an expected result, because during the coarsening process the precipitates increase in size while the number density of the precipitates decreases.

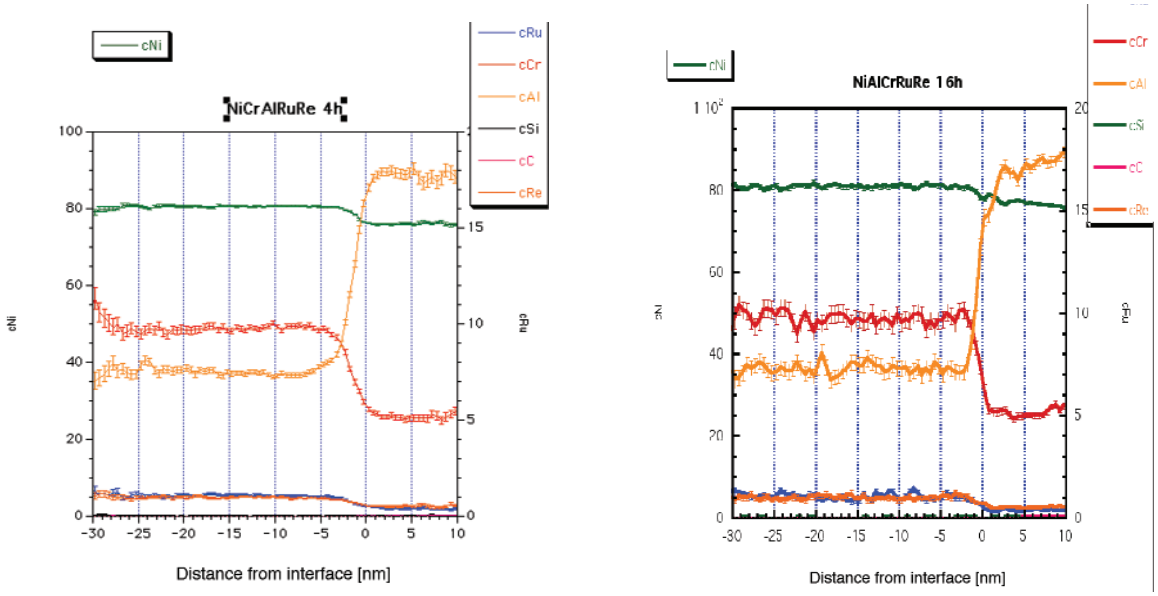

Figure 3: Proximity histograms for the Ni-8.5Cr-10Al-1Ru-1Re alloy.

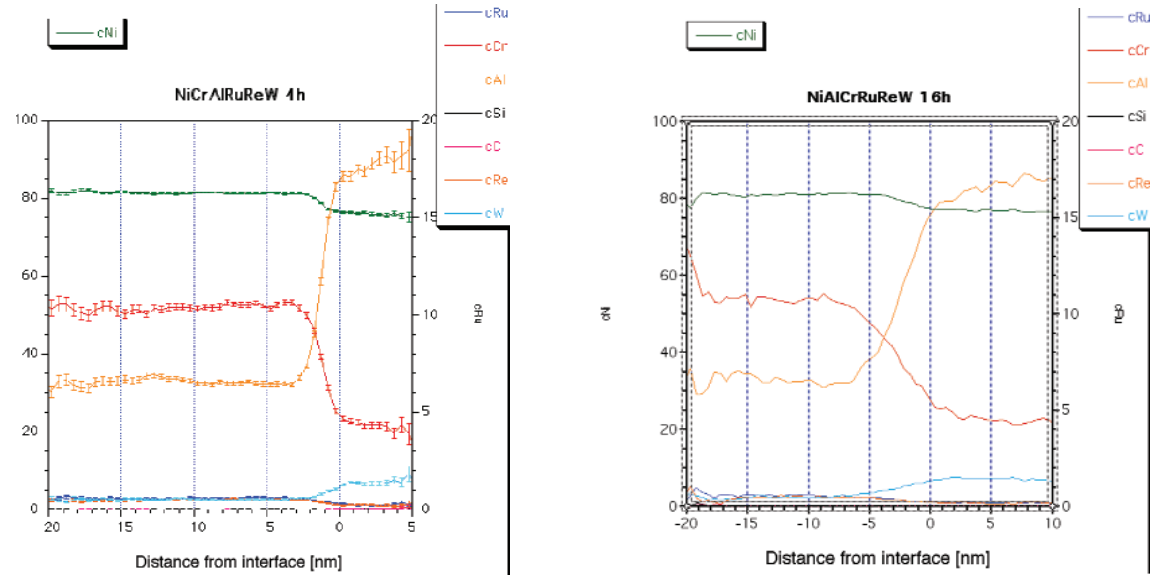

Figure 4: Proximity histograms for the Ni-8.5Cr-10Al-0.5Ru-0.5Re-1W alloy.

Summary and Conclusions

Using 3DAP, the temporal evolution of the nanoscale structures (gamma prime precipitates) in the Ni-8.5Cr-10Al-2Ru at%, Ni-8.5Cr-10Al-1Ru-1Re at%, and Ni-8.5Cr-10Al-0.5Ru-0.5Re-1W at% alloys was investigated. The influence of Ru, Re, and W on the nanostructure, coarsening, and partitioning behavior was studied.

- In the three alloys studied with the 3DAP, the following partitioning behavior was observed: W and Al partition to the precipitate, while Re, Ru, and Cr partition to the matrix.
- At the concentrations studied, the addition of Re to the NiCrAlRu alloy had little influence on the partitioning ratios of Cr and Ru.
- At the concentrations studied, the addition of W to the NiCrAlRuRe alloy did not affect the partitioning ratios of Re and Ru but did cause stronger partitioning of Cr to the matrix and Al to the precipitate.
- Precipitate size increased as a function of time, as shown through comparison of the three-dimensional atom probe data reconstructions.
- Using AFM, the spatial distribution of the nanoscale structure (gamma prime precipitates) in the Ni-8.5Cr-10Al alloy was studied.
- The AFM was able to image shorter aging times than the SEM.
- The number densities as calculated from the AFM images decreased as a function of time. AFM results were in good agreement with previous experiments by TEM and SEM.

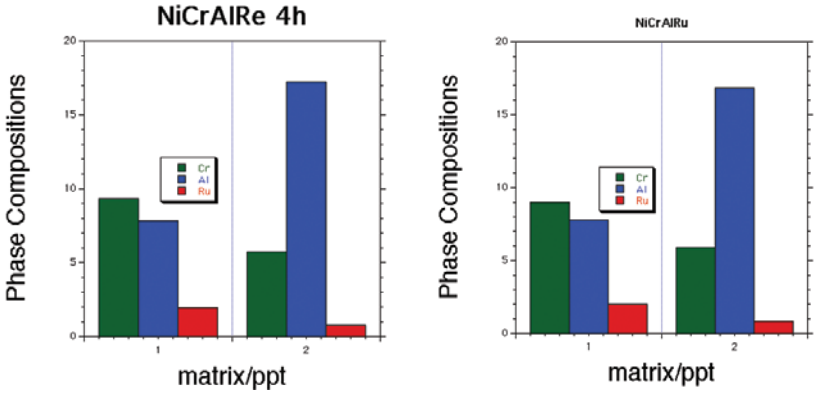

Figure 5: Phase compositions for Ni-8.5Cr-10Al-2Ru. The top graph is 4-hour aging time, and the bottom graph is 16-hour aging time.

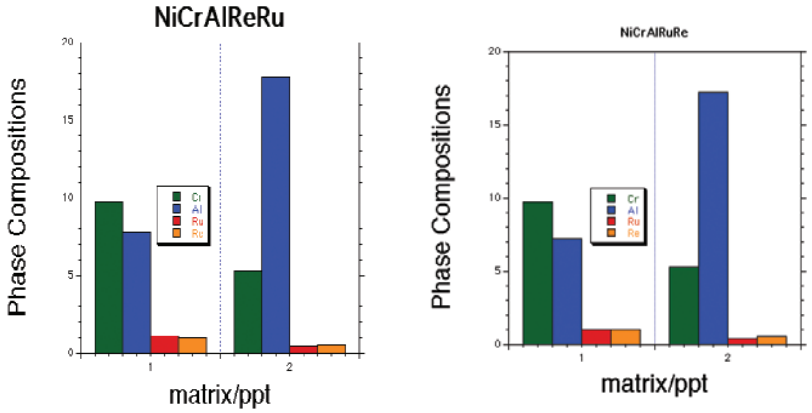

Figure 6: Phase compositions for Ni-8.5Cr-10Al-1Ru-1Re. The top graph is 4-hour aging time, and the bottom graph is 16-hour aging time.

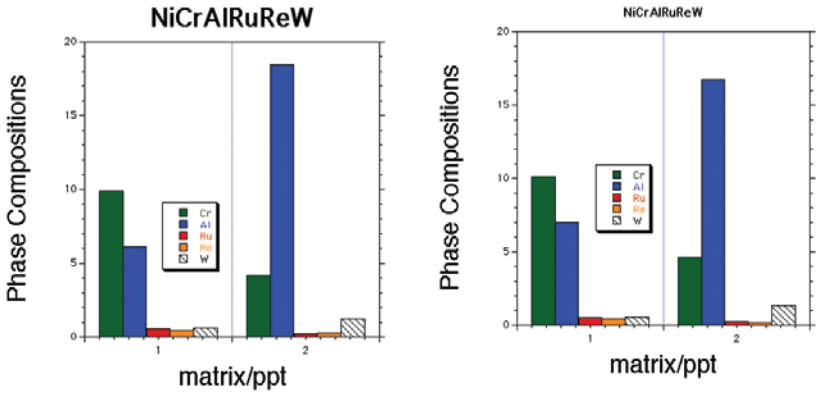

Figure 7: Phase compositions for Ni-8.5Cr-10Al-0.5Ru-0.5Re-1W. The top graph is 4-hour aging time, and the bottom graph is 16-hour aging time.

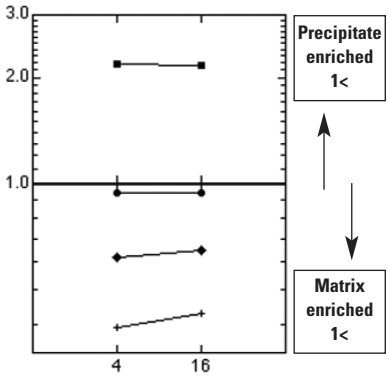

Figure 8: Partitioning ratios of each element in the NiCrAlRu alloy.

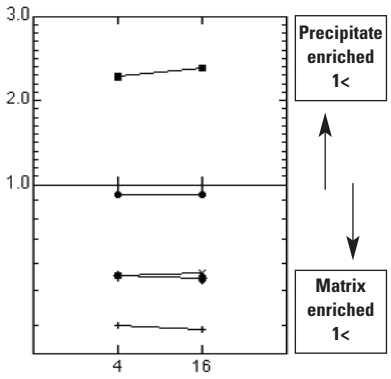

Figure 9: Partitioning ratios of each element in the NiCrAlRuRe alloy.

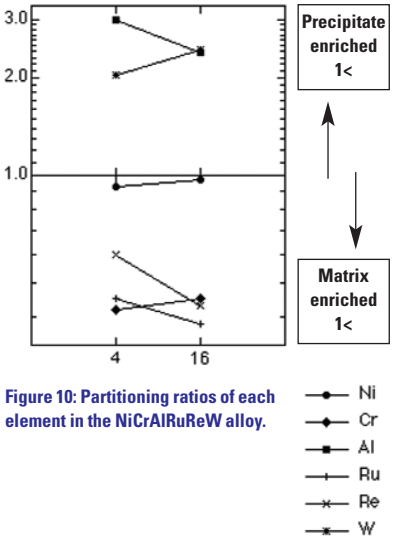

Figure 10: Partitioning ratios of each element in the NiCrAlRuReW alloy.

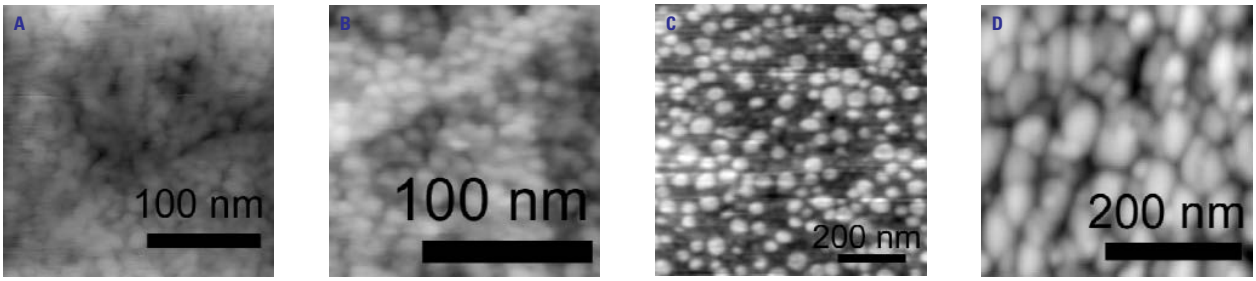

Figure 11: AFM images for Ni-8.5Cr-10Al. (From left to right) A. as quenched (zero hour), B. 15 min, C. one hour, D. four hours.

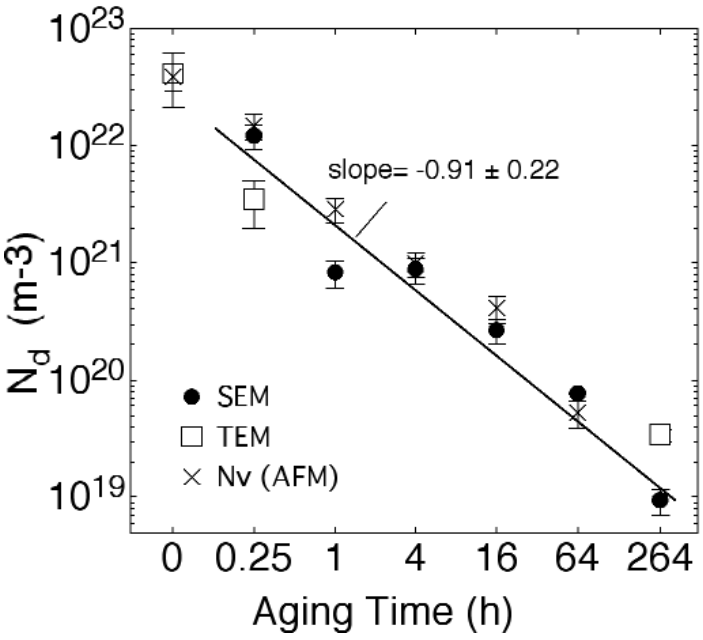

Figure 12: Precipitate number density vs. aging time plot for the Ni-8.5Cr-10Al alloy.

References

(1) Elsevier; http://www.elsevier.com/mrwclus/15/149/40/index.htt, August 2003.

(2) Durard-Charre, M. *The Microstructure of Superalloys.* Gordon and Breach Science: Amsterdam, 1997.

(3) Jena, A. K.; Chaturvedi, M. C. *Mat. Sci.* **1984**, *19*, 3121–39.

(4) Nathal, M. V.; Ebert, L. J. *Met. Trans. A.* **1985**, *16*, 1849–62.

(5) Blavette, D.; Caron, P.; Khan, T. *Scr. Met. Mater.* **1986**, *20*, 1395–1400.

(6) Warren, P. J.; Cerezo, A.; Smith, G. D. W. *Mat. Sci. Eng. A* **1998**, *250*, 88–92.

(7) Sudbrack, C. K.; Isheim, D.; Noebe, R. D.; Jacobson, N. S.; Seidman, D. N. Proceedings Microscopy and Microanalysis 2002, Microscopy and Microanalysis, Volume 8, Supplement 2, 2002, pp. 1098CD–1099CD.